Supporting Information

Zimmermann et al. 10.1073/pnas.1115387108

SI Materials and Methods

Behavioral Assays. *Paw flick.* Noxious heat thresholds were determined according to the Hargreave's test (1). Three consecutive measurements were averaged.

Cold plate. A cold plate (0 °C) was used to assess aversive behavior in response to noxious cold. The amount of flinching, shaking, and paw lifting was counted over 5 min.

Von Frey thresholds. Mechanical sensitivity was determined using calibrated Von Frey fibers. Fibers were applied through a mesh floor, six times each in ascending order of force, until a response (paw withdrawal, shaking or biting, jumping) was elicited. Percent responses were calculated for each fiber application.

Temperature choice assay. A two-plate assay was constructed by joining separately controlled quadratic Peltier plates. An opaque Plexiglas rectangular box formed semidivided chambers of equal size. The behavior of the mice was videotaped, and the time spent on each side was analyzed over 5 min.

Dorsal Root Ganglion Neuronal Cultures and Ca^{2+} Measurements. Adult mice were euthanized by CO_2 inhalation. Dorsal root ganglions (DRGs) from all spinal levels were removed and incubated in 0.6 mg/mL collagenase (Sigma) and 3 mg/mL protease (Sigma) for 30 min at 37 °C in DMEM supplemented with 5 mg/100 mL gentamicin. Ganglia were triturated with a glass pipette, and neurons were plated onto borosilicate glass coverslips (Electron Microscopy Sciences) previously treated with poly-D-lysine (0.1 mg/mL) for 1 h (Sigma). Cells were cultured (37 °C, 5% CO_2) in serum-free TNB-100 base medium (Cedarlane), supplemented with 50 μg/mL penicillin/streptomycin (Invitrogen) and 100 ng/mL nerve growth factor-7S (Alomone). Calcium imaging/patch clamp recordings were made after ∼15–18 h in culture. DRGs were loaded with 15 μM Fura2-AM (Invitrogen) dissolved in TNB medium (for 60–70 min) followed by a 15-min washout in TNB medium. Ca^{2+}-dependent fluorescence transients were recorded in response to perfusion of cold solutions at defined temperatures. Cells were excited with 340 and 380 nM light, and emissions >510 nM were captured by a CCD camera. Intracellular Ca^{2+} ratios (2) were calculated using Slidebook software (Olympus). Cells were considered menthol responsive (250 μM), capsaicin responsive (10 μM), or allyl isothiocyanate-responsive (100 μM) when Ca^{2+} increased >25% above baseline. Cells were considered cold sensitive when Ca^{2+} increased >15% above baseline (apparent Ca^{2+} fluorescence decreased by 5–10% in cold-insensitive cells during cold stimulation). To prepare compounds, menthol (Sigma) was dissolved in ethanol and stored at −20 °C at 0.1M. Capsaicin and allyl isothiocyanate were stored in ethanol:DMSO (1:1) at −20 °C.

Patch Clamp Recordings. HM1 cells (HEK293 cells stably expressing human muscarinic M1 receptor) were maintained in DMEM/F12 (1:1), supplemented with 10% FBS and 10,000 U/mL penicillin/streptomycin in 5% CO_2. Carboxyl-terminal–tagged mouse transient receptor potential (TRP) cation channel, subfamily C member 5 (TRPC5)-EGFP and TRP channel subfamily C, member 1 (TRPC1)-YFP were transiently transfected using Lipofectamine 2000 (Invitrogen). Cells were recorded 24–48 h after transfection. Recordings were performed at defined temperatures (3) in extracellular solution containing (in mM): 140 NaCl, 5 KCl, 2 $CaCl_2$, 1 $MgCl_2$, 10 Hepes, and 10 glucose (adjusted to pH 7.4 with NaOH). The pipette (intracellular) solution contained (in mM): 120 Cs-Mes, 10 Cs_4-BAPTA, 10 Hepes, 2 Mg-ATP, 0.4 Na_2-GTP, 0.47 $MgCl_2$, and 3.26 $CaCl_2$. Whole-cell recordings were acquired at 5 kHz and low-pass filtered (eight-pole Bessel) at 2 kHz. Capacity current was reduced using amplifier circuitry; series resistance compensation was set to 60–80%. Pipettes were heat-polished to a final resistance of 1.3–1.8 MΩ. Carbachol and lanthanum (Sigma) were prepared as stock solutions in distilled water and stored at −20 °C. Temperature coefficients (Q_{10}) were estimated by plotting log (I/I_{max}) vs. temperature. Statistical data are presented as mean ± SEM. Student's t test was calculated, and $P < 0.05$ was considered statistically significant.

Single Nerve Fiber Electrophysiology. The isolated skin saphenous nerve preparation and single-fiber recording technique was used (4, 5) on male littermates of WT and *TRPC5*$^{-/-}$ mice ($n = 32$) weighing 20–32 g and on 129S1/SvImJ mice ($n = 17$) (Jackson Labs).

Mechanosensitive C- and A-fibers. Mechanical probing identified C- and A-fibers. Heat and cold stimulation were applied as previously described (4). Heat ramps from 30–50 °C were applied over 20 s. A discharge of at least two spikes identified heat responsiveness in a mechanosensitive fiber [C-mechano-heat (CMH), polymodal nociceptor]. The noxious heat threshold was set as the temperature of the first spike discharged. In fibers with ongoing activity before heat stimulation, the threshold value was the bath temperature. Temperature was cooled from 30 °C to ∼10 °C over 60 s. The criteria for assigning cold responsiveness [C-mechano-cold (CMC), cold nociceptor] and cold and heat responsiveness [C-mechano-cold-heat (CMCH), multimodal nociceptor] was a discharge of at least three spikes within one period of stimulation in a mechanosensitive C-fiber and a discharge of at least three spikes within two periods of stimulation in A-fibers. The noxious cold threshold was assigned as the first spike during cooling.

Sensitization to cold by menthol. CMC/CMCH-fibers [WT: 21 (of 22), *TRPC5*$^{-/-}$: 19 (of 23)] were treated with 500 μM menthol. Menthol sensitivity was defined as a response when (*i*) the initial control spike number was increased by 20% in response to cold; (*ii*) peak discharge increased by 1.5-fold; or (*iii*) the threshold of activation shifted by ≥2 °C.

Specific cold receptors in C-cold fibers. Specific cold receptors in C-cold (CC)-fibers were identified by response to cold-water stimulus. Electrostimulation and cold stimulation were applied simultaneously to the receptive field to evoke activity-dependent slowing and to distinguish single from multifiber recordings (marking test) (4). In cases of ongoing discharge at 30 °C, the temperature was raised until ongoing discharge ceased, and the temperature at which discharge ceased was defined as the threshold. Nine of 11 WT fibers and 6 of 10 *TRPC5*$^{-/-}$ fibers were treated with menthol. Menthol-induced sensitization resulted in increased adaptation and a prominent shift in dynamic range to warmer temperatures, i.e., inducing discharge at constant warm temperatures at which there was no discharge without menthol (Fig. S5). Wilcoxon matched-pairs (intra-individual) and Mann–Whitney U or χ^2 tests (between groups) were calculated. Differences were considered significant at $P < 0.05$ (Statistica version 6; StatSoft). All results are graphed as mean ± SEM. Skin-nerve electrophysiology experiments were random-choice experiments and therefore not blinded.

Immunolabeling. Cryostat- or paraffin-embedded sections (3–8 μm) were prepared from fresh-frozen or paraformaldehyde-fixed (4%) tissues, respectively. Institutional approval was obtained for the use of existing human samples. For paraffin-embedded sections, deparaffinization and dehydration for 5 min (xylene ×3, 100% ethanol ×2, 95% ethanol ×1, 70% ethanol ×1, and PBS ×1) was followed by boiling slides in Trilogy (Cell Marque) for antigen retrieval and subsequent rinsing in deionized water for 15 min (6). All sections were blocked in 1% BSA and 0.3% Triton X-100 in PBS and were incubated with a variety of previously characterized antibodies (Table S1).

Fluorophore-labeling of mouse monoclonal TRPC5 antibody. We used the mouse monoclonal TRPC5 antibody (NeuroMab) (Table S1), exchanged the buffer to PBS with Econo-Pac 10 DG column (Bio-Rad), and labeled with DyLight 488 Amine-Reactive Dye (Thermo Scientific) according to manufacturer's protocol. Excess dye was removed using the Econo-Pac 10 DG column, and the fluorophore-labeled antibody was concentrated with an Amicon Ultra 10,000 MWCO centrifugal filter.

Immunohistochemistry and fluorescence. Visualization was achieved via HRP-conjugated multimer antibody reagent (Igs; Ventana) in combination with diaminobenzidine as the chromogen (Ultraview; Ventana) or incubation with AlexaFluor 555- or 488-coupled secondary antibodies (Invitrogen). After counterstaining (Hoechst 33258 or hematoxylin), sections were mounted on glass slides and viewed on an epifluorescence-, confocal-, or traditional light microscope.

Quantification. Labeled cells were assessed blinded to genotype and quantified according to previously published protocols (7, 8). For fluorescence microscopy, sections were viewed and quantified using a Zeiss Axiovert 200 inverted fluorescence microscope, an Olympus AX70 epi-fluorescence microscope or were scanned by using a Scancope XT system (Aperio). Image processing was performed using ImageJ (v. 1.37v http://rsb.info.nih.gov/ij/) and Photoshop CS3 (Adobe Systems).

1. Hargreaves K, Dubner R, Brown F, Flores C, Joris J (1988) A new and sensitive method for measuring thermal nociception in cutaneous hyperalgesia. *Pain* 32:77–88.
2. Grynkiewicz G, Poenie M, Tsien RY (1985) A new generation of Ca2+ indicators with greatly improved fluorescence properties. *J Biol Chem* 260:3440–3450.
3. Dittert I, et al. (2006) Improved superfusion technique for rapid cooling or heating of cultured cells under patch-clamp conditions. *J Neurosci Methods* 151:178–185.
4. Zimmermann K, et al. (2009) Phenotyping sensory nerve endings in vitro in the mouse. *Nat Protoc* 4:174–196.
5. Zimmermann K, et al. (2007) Sensory neuron sodium channel Nav1.8 is essential for pain at low temperatures. *Nature* 447:855–858.
6. Cadwell K, et al. (2008) A key role for autophagy and the autophagy gene Atg16l1 in mouse and human intestinal Paneth cells. *Nature* 456:259–263.
7. Hager UA, et al. (2008) Morphological characterization of rat Mas-related G-protein-coupled receptor C and functional analysis of agonists. *Neuroscience* 151:242–254.
8. Lennerz JK, et al. (2008) Calcitonin receptor-like receptor (CLR), receptor activity-modifying protein 1 (RAMP1), and calcitonin gene-related peptide (CGRP) immunoreactivity in the rat trigeminovascular system: Differences between peripheral and central CGRP receptor distribution. *J Comp Neurol* 507:1277–1299.

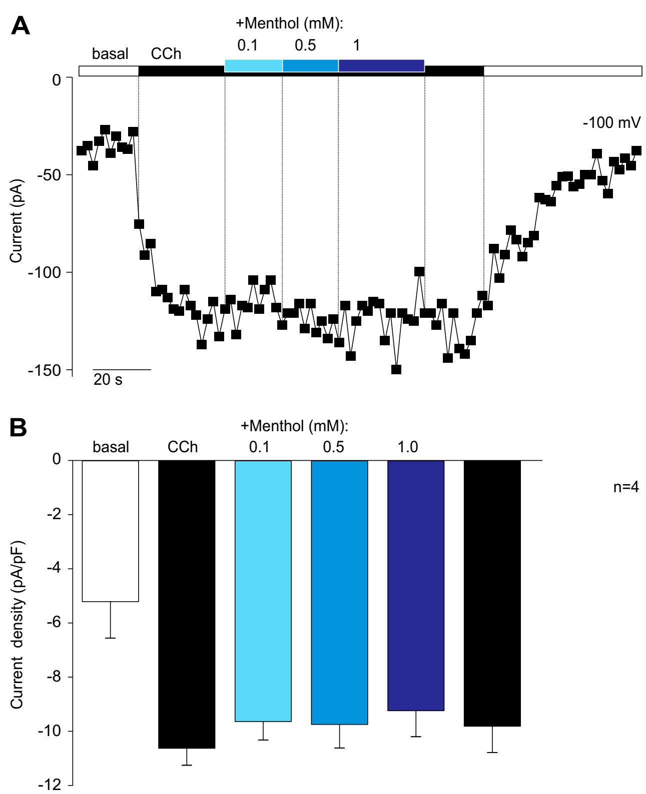

Fig. S1. Sensitivity of TRPC5 to menthol. (*A*) To determine the effects of menthol on TRPC5, we recorded currents from TRPC5- and M1-expressing HEK cells in response to 100 μM carbachol (CCh) application and then added 0.1 mM, 0.5 mM, or 1.0 mM menthol and 100 μM CCh to the cells. (*B*) No significant change in current density was observed during perfusion of menthol at any concentration we tested ($n = 4$). We noted a trend toward a slight reduction in current density over time, probably resulting from slow desensitization of the channel. The pipette contained a solution (in mM) of 110 Cs-Asp, 2 $MgCl_2$, 6 $CaCl_2$, 10 Cs-BAPTA, 10 Hepes, 4 Mg-ATP, 0.3 Na-GTP, pH 7.2, with CsOH (~350 nM free Ca^{2+}). The bath contained a solution (in mM) of 150 NaCl, 4 KCl, 2 $CaCl_2$, 1 $MgCl_2$, 10 Hepes, 10 glucose, pH 7.4 with NaOH.

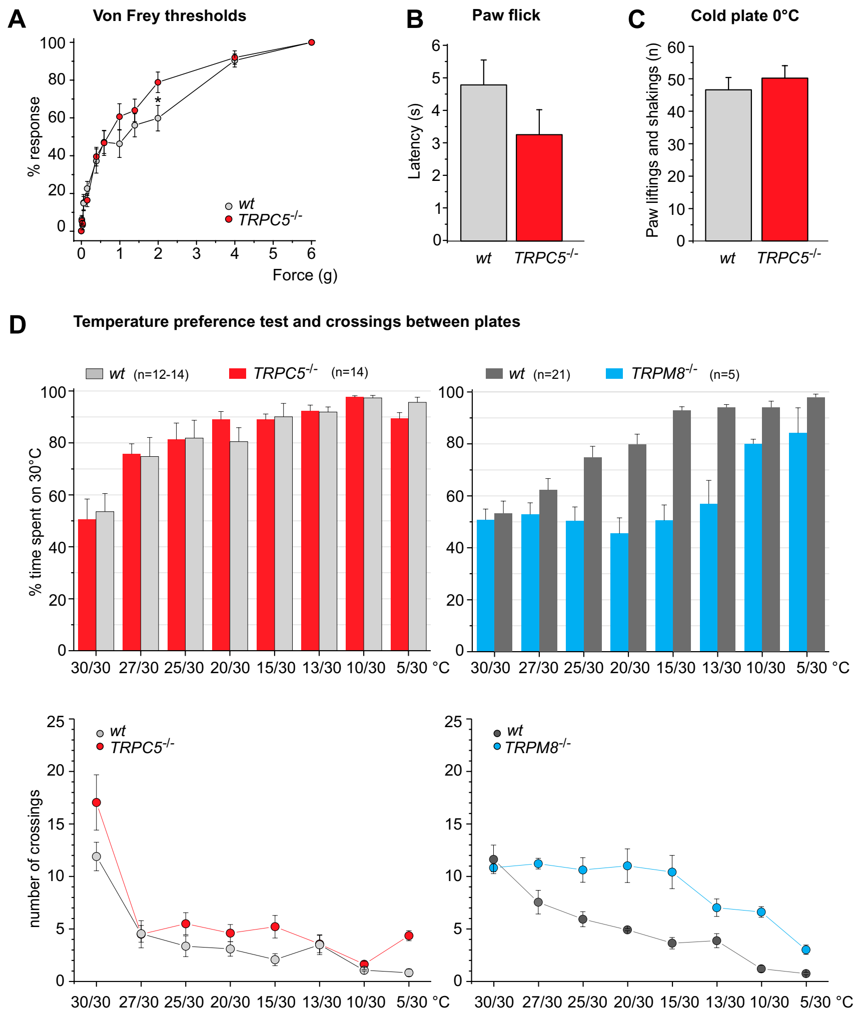

Fig. S2. *TRPC5*-deficient mice have normal temperature preferences and avoidance of cold. (*A*) Thresholds to stimulation with Von Frey fibers were similar in WT (n = 16 animals) and *TRPC5*$^{-/-}$ mice (n = 17 animals). *P_{2g} = 0.03 (Mann–Whitney *U* test). (*B*) Paw-flick latencies to noxious heat irradiation (Hargreave's device) were similar in WT and *TRPC5*$^{-/-}$ mice (n = 10 littermates each). (*C*) Paw liftings and shakings, following placement of mice on a single platform set to 0 °C and counted over 5 min, were similar in *TRPC5*$^{-/-}$ mice (n = 10) and their WT littermates (n = 10). (*D*) Temperature preference behavior in *TRPC5*$^{-/-}$ mice (*Left*) and transient receptor potential menthol receptor 8 knockout (*TRPM8*$^{-/-}$**)** mice (*Right*) and their respective WT littermates were evaluated using the two-plate assay. The percentage of time spent on the 30 °C plate over a 5-min period is shown. The number of crossings between plates per 5-min period was counted and is displayed below the temperature preference graphs. *TRPC5*$^{-/-}$ littermates showed similar preferences and crossings at all temperature differentials examined. For comparison, *TRPM8*$^{-/-}$ littermates expressed temperature preferences and crossings as previously described (14, 15).

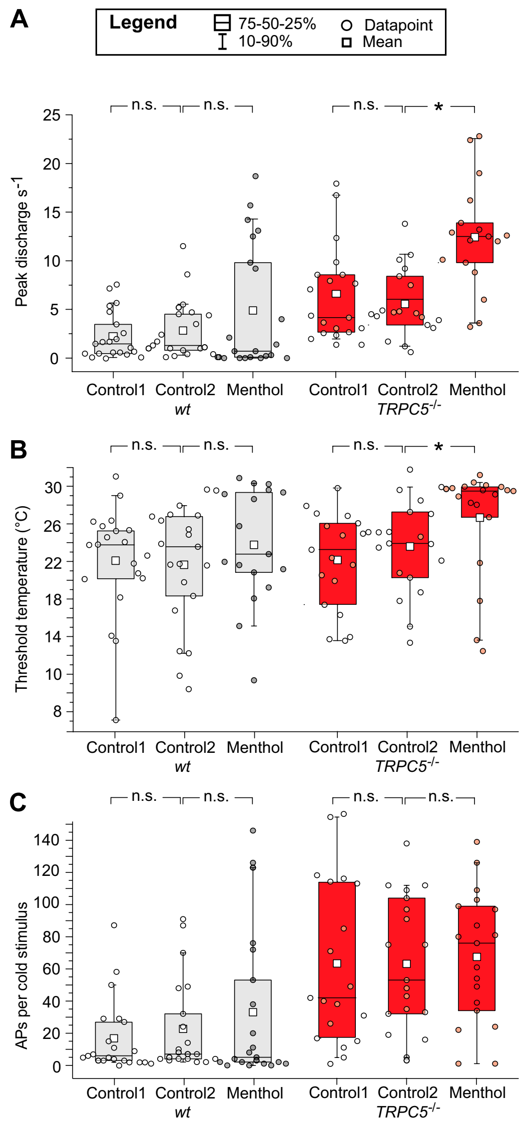

Fig. S3. Sensitization to cold by menthol in CMC- and CMCH-fibers of WT and *TRPC5*$^{-/-}$ *mice*. (*A*–*C*) Effects of menthol application (500 μM) on three characteristic parameters of the cold response in CMC- and CMCH-fibers. (*A*) Peak firing frequency of two control cold responses quantified as action potentials/s (cold stimulus; 30–5 °C over 60 s) and of the cold response 5 min after menthol treatment. Eight of 21 WT fibers were sensitized to cold by menthol, but the effect was not significant over the whole population [average of the second control cold response (control 2): 2.8 ± 0.66/s; menthol: 4.9 ± 1.4/s; $P = 0.33$, Wilcoxon matched pairs test]. In *TRPC5*$^{-/-}$ fibers, 16 of 19 CMC-fibers were sensitized to menthol (average of control 2: 5.5 ± 0.80/s, menthol: 12.4 ± 1.3/s; $P = 0.009$, Wilcoxon matched-pairs test). (*B*) Threshold temperature of two control cold responses and of the cold response 5 min after menthol treatment. In WT fibers, where 8 of 21 C-fibers were sensitized to cold by menthol, the effect was not significant over the whole population (average of control 2: 21.6 ± 1.4 °C, menthol: 23.8 ± 1.4 °C; $P = 0.11$, Wilcoxon matched-pairs test). In *TRPC5*$^{-/-}$ fibers, where 16 of 19 CMC-fibers were sensitized by menthol, the effect was significant (average of control 2: 23.6 ± 1.15 °C, menthol: 26.7 ± 1.3 °C; $P = 0.009$, Wilcoxon matched-pairs test). (*C*) Magnitude of two control cold responses quantified as action potentials/cold stimulus (30–5 °C over 60 s) and of the cold response 5 min after menthol treatment. Although the cold responses were much larger in *TRPC5*$^{-/-}$ fibers than in WT fibers, neither of the genotypes displayed a significant menthol-induced increase in the cold response, most likely because of mixed sensitizing and desensitizing effects of the compound in the native preparation.

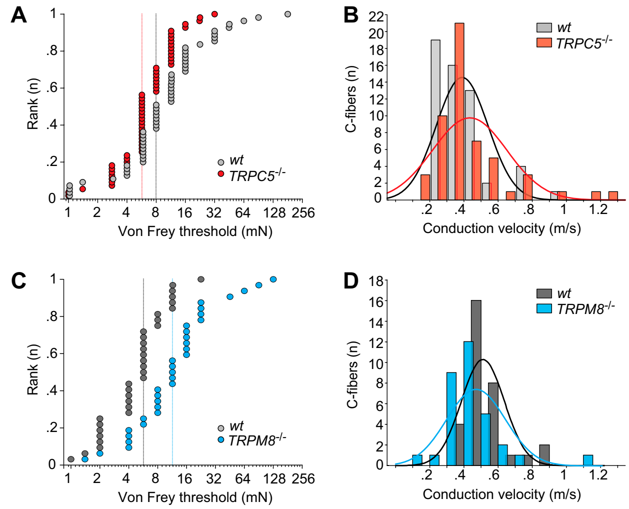

Fig. S4. Von Frey thresholds and conduction velocities in WT, *TRPC5*- and *TRPM8*-null mice. (*A*) Von Frey thresholds of all CM-fibers of WT and *TRPC5*$^{-/-}$ mice (n = 55 each). CM-fibers from *TRPC5*$^{-/-}$ mice displayed lower thresholds than fibers from WT mice, exhibiting a leftward shift of the curve (from 8 mN in WT mice to 5.7 mN in *TRPC5*$^{-/-}$ mice; P = 0.01; Mann–Whitney U test). The lower Von Frey thresholds of *TRPC5*$^{-/-}$ CM-fibers did result in a detectable phenotype in behavioral experiments (compare Fig. S2*A* at 2 g). (*B*) C-fiber conduction velocities for WT and *TRPC5*$^{-/-}$ fibers have a Gaussian distribution with average velocities of 0.43 ± 0.22 m/s and 0.39 ± 0.15 m/s, respectively (P = 0.33; Mann–Whitney U test). (*C*) Von Frey thresholds of all WT and *TRPM8*$^{-/-}$CM-fibers (n = 32 each). CM-fibers from *TRPM8*$^{-/-}$ mice displayed higher thresholds than those from WT mice, exhibiting a rightward shift of the curve (from 5.7 mN in WT mice to 11.4 mN in *TRPM8*$^{-/-}$ mice; P = 0.0002). (*D*) C-fiber conduction velocities for WT and *TRPM8*$^{-/-}$ fibers have a Gaussian distribution with average velocities of 0.51 ± 0.13 m/s and 0.47 ± 0.17 m/s, respectively.

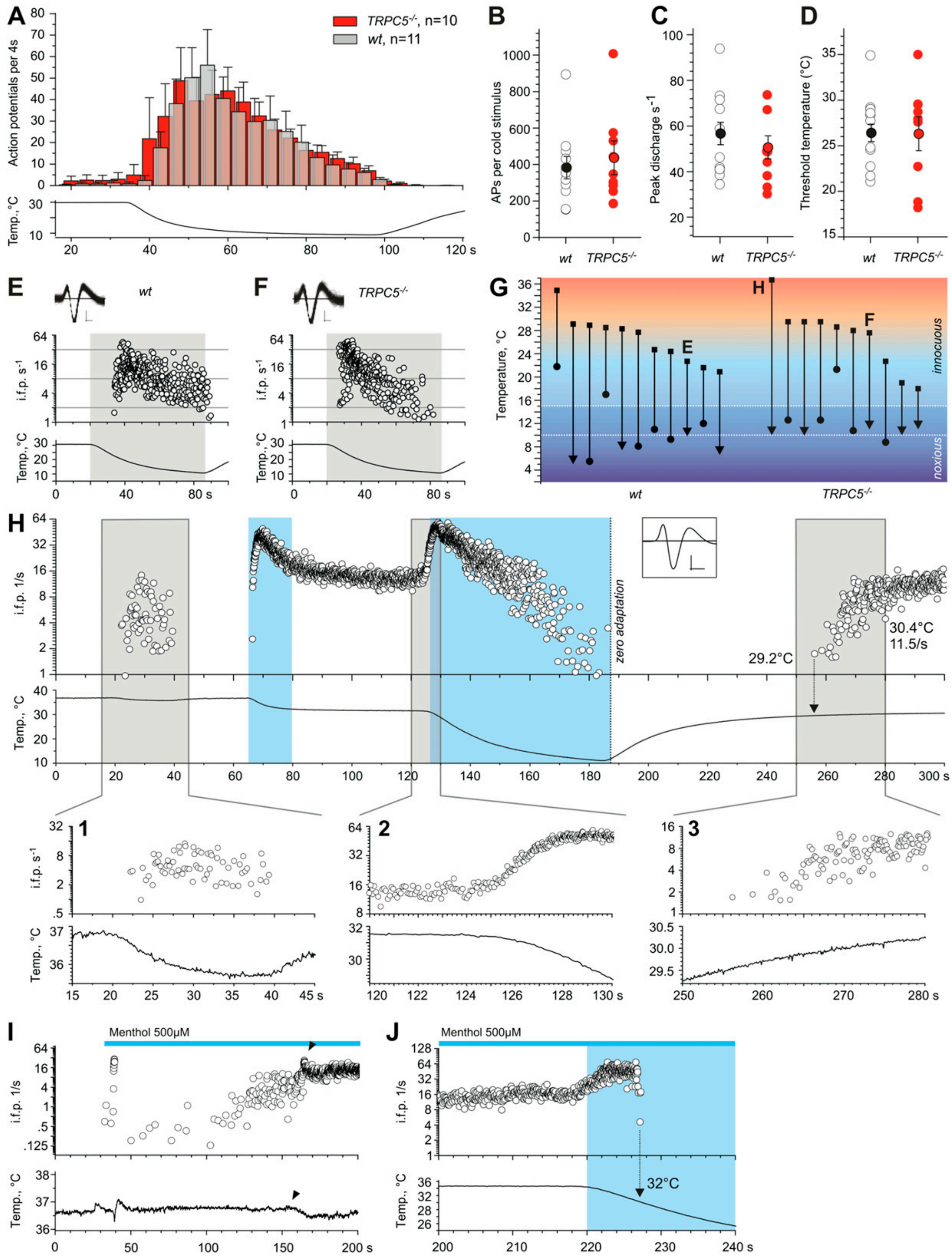

Fig. S5. Cold responses of cold receptor (CC) fibers in WT and *TRPC5*$^{-/-}$ mice. (*A*) Averaged histogram summarizing the cold responses of specific cold receptors (CC-fibers) in both genotypes in bins of 4 s (WT: *n* = 11; *TRPC5*$^{-/-}$: *n* = 10). The lower trace illustrates the time course of the cold stimulus, and whiskers represent SEM. Cold responses did not differ in the two genotypes. (*B*) Action potentials per 60-s cold stimulus in CC-fibers [WT (*n* = 11): 383 ± 62 spikes per cold stimulus; *TRPC5*$^{-/-}$(*n* = 10): 437± 83 spikes per cold stimulus]. (*C*) Peak firing rates of CC-fibers (WT: 57 ± 6 spkes/s; *TRPC5*$^{-/-}$: 51 ± 5 spikes/s). (*D*) Temperature thresholds of cold responses of CC-fibers (WT: 26.6 ± 1.2; *TRPC5*$^{-/-}$: 26.8 ± 1.7). (*E* and *F*) Cold responses of (*E*) representative WT and (*F*) *TRPC5*$^{-/-}$ CC-fiber recordings. Lower traces illustrate time course of cold stimulus. I.f.p. s^{-1}, instantaneous frequency plot. (*Insets*) Extracellular potentials; *y* = 200 µV, *x* = 1 ms. (*G*) Dynamic range of all CC-fibers. Closed squares represent temperature thresholds; closed circles mark fast adaptation to zero and indicate the temperature where the last spike was registered; arrowheads indicate that the dynamic range of the CC-fiber exceeded the stimulus temperature range. Note that 86% of

Legend continued on following page

these CC-fibers are able to encode at or below the noxious cold threshold (indicated as a band between 10–15 °C). (*E*, *F*, and *H* give data for individual fibers illustrated in the respective panels of Fig. S6.) (*H–J*) Recording of a cold receptor with a large dynamic range, slow adaptation properties, and menthol sensitivity (*TRPC5*$^{-/-}$, conduction velocity = 0.47 m/s, threshold temperature = 36.6 °C). (*H*) Instantaneous frequency plot (I.f.p. s^{-1}) shows the response of the thermosensor to temperature changes. Each dot represents one action potential; lower traces indicate the time course of the cold stimulus. Blue columns indicate cold stimulation; gray columns numbered *1–3* mark time frames expanded in three lower graphs. (*1*) The highly dynamic response pattern of this receptor class is illustrated: A temperature change of −0.25 °C leads to a phasic response at high rates (8–16/s). (*2*) Static and dynamic response pattern of CC-fibers with distinctively graded static discharge at any temperature within the dynamic range (e.g., 11.5/s at 30.4 °C and 12.9/s at 31.6 °C, averaged over >1 min). (*3*) Rewarming from a cold stimulus leads to immediate zero adaptation (dotted line at ∼185 s in graph H, zero adaptation), whereas a small temperature gradient leads to unchanged activity (arrow at ∼255 s). (*I* and *J*) The response pattern to the application of menthol. (*Inset)* Average spike shape of the response (n = 2,384 action potentials; SD = ±0.57; y = 200 μV, x = 1 ms). (*I*) Application of menthol led to excitation at 36.6 °C (threshold temperature) and an increased sensitivity to small negative temperature changes (arrowheads). (*J*) Strong increase in adaptation to cold stimulation. Note zero adaptation at 32 °C (arrow).

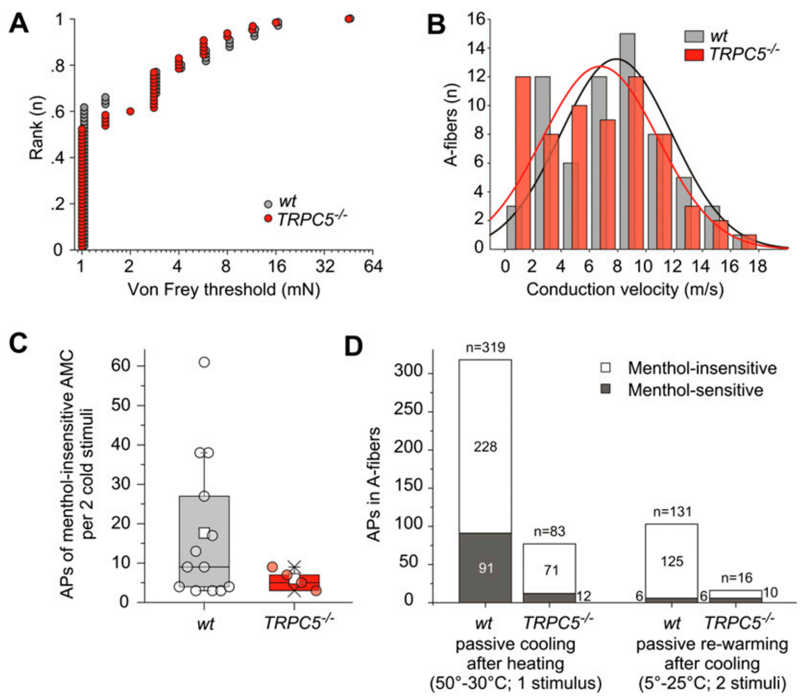

Fig. S6. Loss of function in Aδ-cold nociceptors (AMC) in WT and *TRPC5*$^{-/-}$ fibers. (*A*) Von Frey thresholds of all Aδ-mechanosensitive (AM) WT and *TRPC5*$^{-/-}$ fibers (n = 65 each). Thresholds are ranked from low to high; median = 1 mN. (*B*) Conduction velocity histogram of all Aδ-fibers is Gaussian with average WT velocities of 6.71 ± 0.5 m/s and average *TRPC5*$^{-/-}$ velocities of 6.04 ± 0.5 m/s. (*C*) Response magnitude of all cold-sensitive menthol-insensitive Aδ-fibers shown in main Fig. 4*I*. (*D*) (*Left*) Cumulative number of action potentials (APs) during 60 s of passive cooling from 50°–30 °C after heat stimulation (n = 65 fibers per genotype). (*Right*) Number of action potentials discharged during two periods of rewarming to skin temperature from a cold stimulus (∼5–30 °C; n = 65 fibers per genotype).

Table S1. Primary antibodies

Name	Host	Antigen characteristics	Catalog no.; source	Dilution	Reference
Neurofilament heavy chain (NF200)	Rb; p	Full-length native protein	ab8135; Abcam, Cambridge, MA	M1:1000	(1, 2)
Peripherin	Ck; p	Recombinant protein expressed in bacteria	ab39374; Abcam, Cambridge, MA	M1:500H1:50	(3)
Calcitonin gene-related peptide (CGRP)	Rb; p	Synthetic rat α-CGRP	T-4032; Bachem Group, Peninsula Labs, San Carlos, CA	M1:1000	(4)
TRPV1	Gp; p	C terminus of rat TRPV1 (YTGSLKPEDAEVFKDSMVPGEK)	GP14100; Neuromics, Edina, MN	M1:1000	(5, 6)
TRPM8	Rb; p	short peptide of N terminus of TRPM8	KAL-KM060; CosmoBio, Carlsbad, CA	M1:500H1:50	(7, 8)
TRPC5*	Ms; m	Synthetic peptide; aa 827–845 of human TRPC5 (SKAESSSKRSFMGPSLKKL)	75–104; NeuroMab, Davis, CA	H1:200	(9, 10)
TRPC5	Rb; p	Peptide; aa 9590973 of human TRPC5 (C)HKWGDGQEEQVTTRL	ACC-020; Alomone Labs Ltd, Jerusalem, Israel	M1:2000	(11)
PGP9.5	Rb; p	Recombinant human UCH-L1 (full length native protein)	AB1761, Millipore Corporation	H1:2000	(12, 13)
PGP9.5	Gp; p	Full-length native protein	ab5898; Abcam, Cambridge, MA	H1:200	(14, 15)
Isolectin B4 (IB4)	N/A	Lectin; Griffonia simplicifolia B4 subunit binding to α-D-galactosyl residues	I21412; Invitrogen, Carlsbad, CA	M1:500	(16, 17)

Ck, chicken; Gp, guinea pig; H, human; M, mouse; m, monoclonal; Ms, mouse; p, polyclonal; PGP9.5, protein gene product 9.5; Rb, rabbit; TRPV1, TRP receptor potential cation channel subfamily V member 1.

*The NeuroMab antibody was labeled directly to eliminate nonspecific staining (*SI Materials and Methods*).

1. Girard C, et al. (2008) Etifoxine improves peripheral nerve regeneration and functional recovery. *Proc Natl Acad Sci USA* 105:20505–20510.
2. Harris J, Ayyub C, Shaw G (1991) A molecular dissection of the carboxyterminal tails of the major neurofilament subunits NF-M and NF-H. *J Neurosci Res* 30:47–62.
3. McLean J, et al. (2010) Distinct biochemical signatures characterize peripherin isoform expression in both traumatic neuronal injury and motor neuron disease. *J Neurochem* 114(4): 1177–1192.
4. Lennerz JK, et al. (2008) Calcitonin receptor-like receptor (CLR), receptor activity-modifying protein 1 (RAMP1), and calcitonin gene-related peptide (CGRP) immunoreactivity in the rat trigeminovascular system: Differences between peripheral and central CGRP receptor distribution. *J Comp Neurol* 507:1277–1299.
5. Caterina MJ, et al. (1997) The capsaicin receptor: A heat-activated ion channel in the pain pathway. *Nature* 389:816–824.
6. Guo A, Vulchanova L, Wang J, Li X, Elde R (1999) Immunocytochemical localization of the vanilloid receptor 1 (VR1): Relationship to neuropeptides, the P2X3 purinoceptor and IB4 binding sites. *Eur J Neurosci* 11:946–958.
7. Bautista DM, et al. (2007) The menthol receptor TRPM8 is the principal detector of environmental cold. *Nature* 448:204–208.
8. Obata K, et al. (2005) TRPA1 induced in sensory neurons contributes to cold hyperalgesia after inflammation and nerve injury. *J Clin Invest* 115:2393–2401.
9. Gomis A, Soriano S, Belmonte C, Viana F (2008) Hypoosmotic- and pressure-induced membrane stretch activate TRPC5 channels. *J Physiol* 586(Pt 23):5633–5649.
10. Riccio A, et al. (2009) Essential role for TRPC5 in amygdala function and fear-related behavior. *Cell* 137(4):761–772.
11. Facemire CS, Mohler PJ, Arendshorst WJ (2004) Expression and relative abundance of short transient receptor potential channels in the rat renal microcirculation. *Am J Physiol Renal Physiol* 286(3):F546–F551.
12. Thompson RJ, Doran JF, Jackson P, Dhillon AP, Rode J (1983) PGP 9.5–A new marker for vertebrate neurons and neuroendocrine cells. *Brain Res* 278(1-2):224–228.
13. Wilson PO, et al. (1988) The immunolocalization of protein gene product 9.5 using rabbit polyclonal and mouse monoclonal antibodies. *Br J Exp Pathol* 69(1):91–104.
14. Day IN, Hinks LJ, Thompson RJ (1990) The structure of the human gene encoding protein gene product 9.5 (PGP9.5), a neuron-specific ubiquitin C-terminal hydrolase. *Biochem J* 268(2): 521–524.
15. Navarro X, Verdu E, Wendelschafer-Crabb G, Kennedy WR (1997) Immunohistochemical study of skin reinnervation by regenerative axons. *J Comp Neurol* 380(2):164–174.
16. Li H, Nomura S, Mizuno N (1997) Binding of the isolectin I-B4 from Griffonia simplicifolia to the general visceral afferents in the vagus nerve: A light-and electronmicroscope study in the rat. *Neurosci Lett* 222(1):53–56.
17. Wang HF, Robertson B, Grant G (1998) Anterograde transport of horseradishperoxidase conjugated isolectin B4 from *Griffonia simplicifolia* I in spinal primary sensory neurons of the rat. *Brain Res* 811(1-2):34–39.

Table S2. Immunohistochemical analysis of pairs of WT and *TRPC5*$^{-/-}$ lumbar DRG neurons

Marker	*TRPC5* genotype	Total neurons	Positive neurons	Percentage ± SEM
NF200 (*n* = 1)	+/+	3,152	1,293	41.0 ± 1.6
	–/–	3,234	1,331	41.2 ± 1.5
Peripherin (*n* = 1)	+/+	2,819	1,062	56.8 ± 1.3
	–/–	3,325	1,882	56.6 ± 1.4
CGRP (*n* = 1)	+/+	2,073	406	19.6 ± 1.2
	–/–	2,678	577	21.5 ± 1.1
IB4 (*n* = 1)	+/+	3,859	1,134	29.4 ± 1.3
	–/–	3,365	1,055	31.4 ± 1.6
TRPV1 (*n* = 2)	+/+	5,702	1,022	17.9 ± 0.8
	–/–	5,194	844	16.2 ± 0.5
TRPM8 (*n* = 3)	+/+	5,835	1,076	18.2 ± 0.6
	–/–	6,745	739	10.9 ± 0.6

Sensory neurons were labeled for Neurofilament 200 (NF200), Peripherin, IB4, CGRP, TRPV1, and TRPM8 antibodies; *n* indicates number of pairs of lumbar dorsal root ganglia.

Table S3. Functional expression of TRP subtypes in cultured DRG neurons identified by characteristic pharmacological tools

	TRPM8 Menthol (100 μM)		TRPA1 Allyl isothiacyanate (100 μM)		TRPV1 Capsaicin (10 μM)	
Subtype	Sensitive/total neurons	%	Sensitive/total neurons	%	Sensitive/total neurons	%
WT	82/989	8.3	132/333	39.6	112/333	33.6
TRPC5 $^{-/-}$	49/1,022	4.8	102/333	30.6	100/333	30.0

Cultured sensory neurons were subjected to stimulation with TRP channel agonists in calcium imaging.

Table S4. Mechanosensitive C-fiber subtypes in WT, *TRPC5*$^{-/-}$, and *TRPM8*$^{-/-}$ mice

	Fiber types	CM		CMC		CMCH		CMH	
Genotype	Total *n*	*n*	%	*n*	%	*n*	%	*n*	%
TRPC5$^{+/+}$	55	16	29	16	29	6	11	17	31
TRPC5$^{-/-}$	55	14	25	22	40	1	2	18	33
TRPM8$^{+/+}$	32	4	13	8	25	9	28	11	34
TRPM8$^{-/-}$	32	5	16	0	0	8	25	19	59

Criteria for classification of nociceptive C-fibers are described in *SI Materials and Methods*. *TRPM8*$^{-/-}$ mice were generated by Dhaka/Patapoutian and backcrossed on N5 generations onto C57/BL6 background; the different inbred backgrounds may entail strain differences in fiber subtypes. Note the lack of CMC-fibers in *TRPM8* knockout mice, associated with increased numbers of CMH-fibers; see also Fig. 4*H*.